

Applications of computer simulation, nuclear reactions and elastic scattering to surface analysis of materials

J. A. R. PACHECO DE CARVALHO^{1,2}, A. D. REIS¹

¹U. Det. Remota, ¹Dep. de Física, ²Centro de Informática, Universidade da Beira Interior,
Rua Marquês d'Ávila e Bolama, 6201-001 Covilhã, Portugal.

This article involves computer simulation and surface analysis by nuclear techniques, which are non-destructive. Both the "energy method of analysis" for nuclear reactions and elastic scattering are used. Energy spectra are computer simulated and compared with experimental data, giving target composition and concentration profile information. The method is successfully applied to thick flat targets of graphite, quartz and sapphire and targets containing thin films of aluminium oxide. Depth profiles of ¹²C and ¹⁶O nuclei are determined using (d,p) and (d,α) deuteron induced reactions. Rutherford and resonance elastic scattering of (⁴He)⁺ ions are also used.

Keywords: Thick/thin films, Surfaces, Non-destructive tests, Nuclear reactions, Elastic scattering.

Aplicaciones de simulación por ordenador, reacciones nucleares y difusión elástica al análisis de superficies de materiales

Este artículo trata de simulación por ordenador y del análisis de superficies mediante técnicas nucleares, que son no destructivas. Se usa el "método de análisis en energía" para reacciones nucleares, así como el de difusión elástica. Se simulan en ordenador espectros en energía que se comparan con datos experimentales, de lo que resulta la obtención de información sobre la composición y los perfiles de concentración de la muestra. Este método se aplica con éxito en muestras espesas y planas de grafito, cuarzo y zafiro y muestras conteniendo películas finas de óxido de aluminio. Se calculan perfiles en profundidad de núcleos de ¹²C y de ¹⁶O a través de reacciones (d,p) y (d,α) inducidas por deuterones. Se utiliza también la difusión elástica de iones (⁴He)⁺, tanto a Rutherford como resonante.

Palabras clave: Películas espesas/finas, Superficies, Tests no destructivos, Reacciones nucleares, Difusión elástica.

1. INTRODUCTION

The importance of the field of material analysis has been recognized worldwide for its implications on the progress of a wide range of human activities. Very considerable scientific efforts have been concentrated on the development of techniques capable of providing information on solid materials. A large part has been on ion, electron and photon beams interacting with a solid target. Surface analysis techniques permit target information to be gained for a range of depths near the surface. A wide range of such techniques has been available. The techniques are complementary. There are nuclear and non-nuclear techniques. Elastic scattering, nuclear reactions and ion-induced X-rays are the main nuclear surface analysis techniques. They are non-destructive and capable of providing analysis for a few microns near the surface. Many applications have been made such as in industry, scientific and medical areas. Nuclear reactions and elastic scattering are the more precise techniques for obtaining absolute values of concentrations in surface analysis. Low energy ion accelerators, for MeV ion beams, have been used for new applications, for surface analysis (1,2). Through nuclear reactions not only high sensitivities are possible for

detection of light elements in heavier substrates, but also discrimination of isotopes of the same element. Each reaction is specific of an isotope. In both the "energy method of analysis" for nuclear reactions and in elastic scattering, an energy spectrum is acquired of ions emitted from different depths in the sample, for a single energy of an incident ion beam (3-13), as detailed in the present work. Depth profiling of light nuclei such as ¹⁶O and ¹²C, has been reported in several contexts (14,15), including applications in ceramics and glass industry (16,17). In the "energy method of analysis", which is appropriate for ion-ion reactions, the energy spectrum which is acquired, intrinsically contains information about target composition and concentration profiles. This information is computationally gained from the spectrum (4,6,18,19).

2. EXPERIMENTAL

2. EXPERIMENTAL ARRANGEMENT AND SAMPLES

The experimental work was possible through the University of Manchester, England, using a 7 MV Van de Graaff

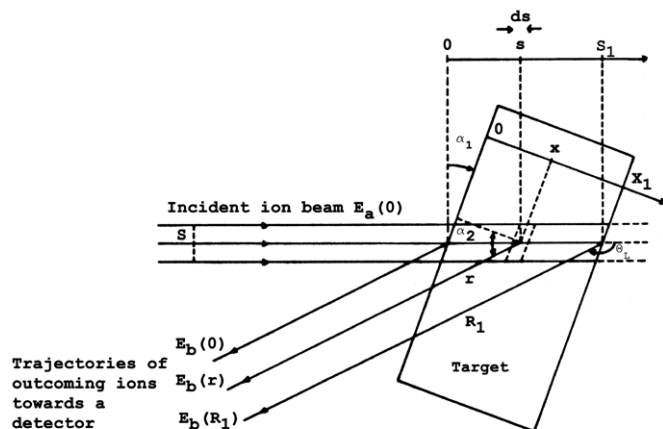


Fig. 1- Schematic representation of a nuclear reaction experiment.

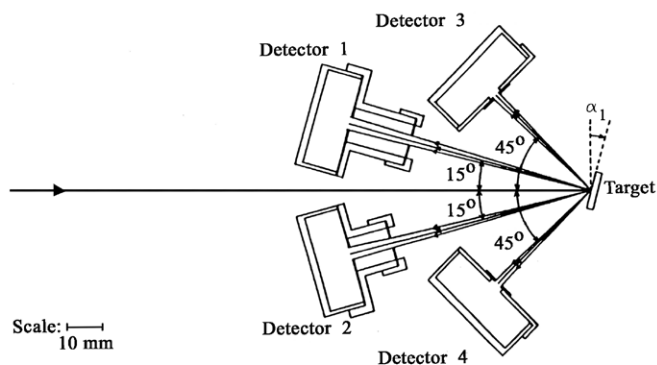


Fig. 2- Representation of the experimental arrangement for detection of charged particles.

accelerator. Given an incident beam of accelerated ions, for an ion-ion nuclear reaction experiment schematically represented in Fig.1, ion detection from the sample at detection angles θ_L of 135° and 165° used silicon surface barrier detectors, chosen as suitable for the reaction and energy ranges involved (6). The experimental arrangement of the detectors is shown in Fig. 2. Spectral data of ions from the sample were acquired through an on-line computer equipped with data acquisition software. Computer data interfaces were connected to chains consisting of charge preamplifiers, amplifiers and analogue to digital converters providing for pulse pile-up rejection. Spectra were acquired as counts per channel versus channel number. Following energy calibration of these spectra, spectral yields as counts per unit energy versus energy were obtained.

We used the following samples as targets for acquisition of charged particle spectra: 1) One thick, high purity, flat sample of pyrolytic graphite; this sample was made by Union Carbide, by cracking CH_4 at 2200°C and depositing onto a graphite substrate. Two thick, high purity, flat samples consisting of compounds of elements, such as oxides; 2) the first was a sapphire sample, labelled Al_2O_3 ; 3) the second was a quartz sample, labelled SiO_2 . 4) A sample designated as Al/ Al_2O_3 , formed by a thin film of Al_2O_3 on a thick high purity flat aluminium substrate; this sample was prepared through aluminium anodization at 100V , 20°C , in a 3% per volume

aqueous solution of tri-ammonium citrate, at pH 6 and a current density of 50 mA cm^{-2} ; this method of preparation was expected to ensure excellent uniformity of the oxide; the figure quoted (20) of 13.7 \AA/V gave for our oxide a nominal thickness of $0.1370\text{ }\mu\text{m}$; transmission electronic microscopy has shown that not only the aluminium substrate was flat, but also the oxide was quite uniform, as given in Fig. 3; from higher magnification pictures obtained with the transmission electron microscope, we determined an oxide thickness of $0.1340\text{ }\mu\text{m}$. 5) Two flat self-supported samples of anodic aluminium oxide; the targets were obtained by aluminium anodization at 100V and 200V in a 3% per volume aqueous solution of tri-ammonium citrate, at 20°C , pH 6 and a current density of 5 mA cm^{-2} ; following anodization of a flat, high purity Al foil, chemical methods were used to leave a 1 cm diameter self-supported oxide window in the foil; the Al anodization procedure mentioned gave nominal thicknesses of $0.1370\text{ }\mu\text{m}$ and $0.2740\text{ }\mu\text{m}$ for anodization at 100V and 200V , respectively (20).

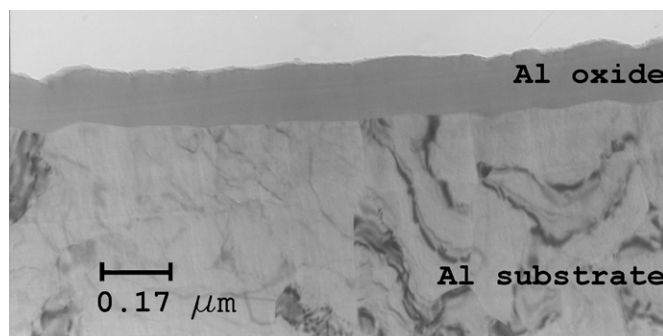


Fig. 3- Transmission electron micrograph of a section of the Al/ Al_2O_3 target.

3. COMPUTER SIMULATION

A large computer program has been developed for simulation of energy spectra of charged particles from nuclear reactions from targets under ionic bombardment (6). Elastic scattering is a particular and important case. The computations mainly account for: target parameters, such as composition and concentration profiles; energy spread of the incident ion beam; geometric factors and target rotation; stopping power; differential cross section; energy straggling; detector resolution. An option permits calculation of effects from: small forward angle multiple scattering; incident beam size and angular divergence; detector angular aperture. For specified parameterization, a predicted spectrum from the target is computed and compared visually with experimental data on a display. The chi-square is calculated, to give an indication of the goodness of fit. If the prediction was far from the data new parameterisation was fed in, giving new predictions. This was repeated until a satisfactory agreement was reached between predictions and the data. The main aim was to gain information about target composition parameters. For this, the main aim was to vary target composition parameters, while other parameterization was kept constant. A predicted spectrum from a given target is obtained by summing predicted basic spectra, each from an ion-ion reaction or from elastic scattering for a concentration distribution of an individual target nuclide. The following parameterization was available

for the computations, which were mainly intended for light ions: 1) Gaussian beam energy profile for a given bombarding energy; as an option, beam size and gaussian distribution of projected angles. 2) Flat thick multi-layered target, allowing for three layers which could vary from very thin to very thick. For each layer, up to four isotopes were considered. Layer thickness parameters were required. For a single element the atomic density was needed. For a mixture of isotopes, the mixture density and the ratios of atomic densities were fed in. For a compound or a mixture of elements the parameterization was similar. The isotopic composition of a given element was possible through the percentages of occurrence of its isotopes. The main types of concentration profiles were: step functions, complementary error functions, exponential functions, linear combinations of error functions. Other types of profiles were possible by feeding in tables of atomic density versus depth. Target rotation was included. 3) Gaussian detector response function. Detection angle. Target to detector distance and detector angular aperture were usable as an option. 4) Rutherford cross section was the default for elastic scattering. Available differential cross section versus energy data, for elastic scattering and nuclear reactions, were used to create the necessary data files to be fed in. 5) The main approach for stopping power versus energy data for single element was from (21,22). Other data were usable to create data files to be fed in, as necessary, containing stopping power versus energy information. For compounds or mixtures Bragg's rule (23) was used to calculate stopping powers. Deviations from this rule were correctable through stopping power scaling factors for each ion type. Therefore, for a nuclear reaction, separate scaling factors were available both for ingoing ions penetrating the target and for outcoming ions travelling towards the detector. 6) Theories for gaussian energy straggling were considered. The default was Bohr theory (24). As the main option, Lindhard-Scharff theory (25) was selectable. Energy straggling factors were allowed, for both ingoing and outcoming ions. Those were intended, if required, to vary within limits close to unity. 7) For targets where each layer was constituted by a single element, an option permits inclusion of angular and lateral spread distributions from small forward angle multiple scattering in the gaussian approximation. The Fermi theory was used (26). The approach given by Bethe and Ashkin (27) was selectable as an option. Allowance was made for multiple scattering factors for both ingoing and outcoming ions.

For calculations of energy losses along paths of the ingoing ions in a layer, a small ingoing energy decrement was fed in. Details of differential cross section data were preserved, as the points in a given tabulation were usable as intermediate points. Up to typically 400 points were usable, depending on array size. For calculations of energy losses along paths of the outcoming ions from a layer, an outcoming energy decrement was automatically selected. Numeric integration and a fast interpolation routine were used, whenever required, e.g. in evaluations of convolution integrals. In building a basic spectrum we considered, in short, calculations of: mean ingoing energies and ingoing energy distributions; depth dependence of the yield, by folding in differential cross section versus energy and ingoing energy distributions; mean energies and energy distributions from nuclear reaction events; mean outcoming energies and outcoming energy distributions; dependence of the yield on mean outcoming energy; dependence of the yield on outcoming energy, by folding in yield versus mean outcoming energy and outcoming energy

distributions; dependence of the yield on detection system resolution, giving final yield versus energy, by folding in yield versus outcoming energy and detector resolution function. In the prediction of a basic spectrum, the calculations were made for unitary incident ion beam dose, unitary solid angle of the detector and unitary detection system efficiency. Therefore, a reference basic spectrum from the surface of the target was multiplied by a scaling factor arising from experimental data. For further predicted basic spectra that scaling factor was taking into account. Normalizations were calculated to ensure correct ratios of total yields of the respective spectral shapes.

4. RESULTS AND DISCUSSION

4.1. Nuclear reactions

In making the predictions for nuclear reactions induced by deuterons, we used available data of stopping power of the ions in the samples (21,22,28,29). For the reactions (d,p) in ^{12}C , (d, α) and (d,p) in ^{16}O we used available data of differential cross sections for these reactions (6,30,20). In particular, the differential cross section data for the $^{12}\text{C}(\text{d},\text{p})^{13}\text{C}$ reaction permitted very good computed fits to spectra from a thick flat, high purity target of pyrolytic graphite for several deuteron bombarding energies of 1.12-1.86 MeV, $\theta_{\text{R}}=4.5^\circ \pm 1^\circ$, and $\theta_{\text{L}}=165^\circ$ and 135° . This is illustrated in Fig. 4 at 1.12 MeV and 165° , where a uniform concentration profile of ^{12}C along $7\text{ }\mu\text{m}$ was used. The quartz sample was analysed through a 1.0 MeV deuteron beam, at normal incidence and $\theta_{\text{L}}=135^\circ$. The choice of the bombarding energy was made to give insignificant yields of deuteron induced reactions in ^{28}Si . The spectrum from the reactions (d,p) in ^{12}C , (d, α) and (d,p) in ^{16}O is shown in Fig. 5. It can be seen that a reasonably good computed fit to the overall data was obtained. A thin surface film of ^{12}C with uniform concentration and thickness $X_1=0.062\text{ }\mu\text{m}$, and a uniform distribution of ^{16}O in the quartz were detected. The ^{16}O thickness parameters X_2 were $3.4\text{ }\mu\text{m}$ for (d, α_0), $5.5\text{ }\mu\text{m}$ for (d,p₀) and $5.2\text{ }\mu\text{m}$ for (d,p₁). For the same target, details of another good computed fit are shown in Fig. 6 to the spectral shape from the $^{16}\text{O}(\text{d},\text{p}_1)^{17}\text{O}^*$ reaction for 0.993 MeV and $\theta_{\text{L}}=135^\circ$, with a thickness parameter X_2 of $5.2\text{ }\mu\text{m}$.

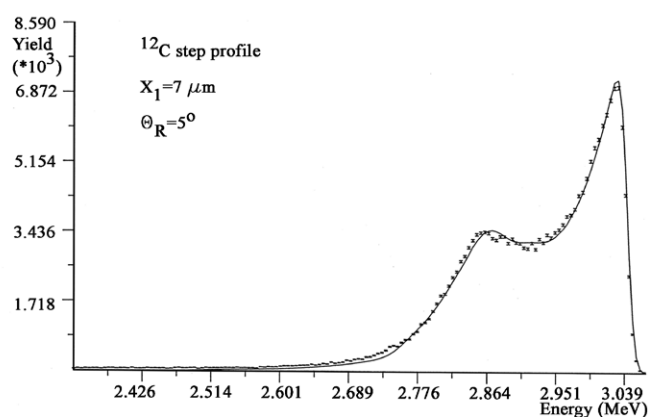


Fig. 4- Computed fit to data of the $^{12}\text{C}(\text{d}, \text{p})^{13}\text{C}$ reaction in the pyrolytic graphite target for $E_d=1.12\text{ MeV}$ and $\theta_{\text{L}}=165^\circ$.

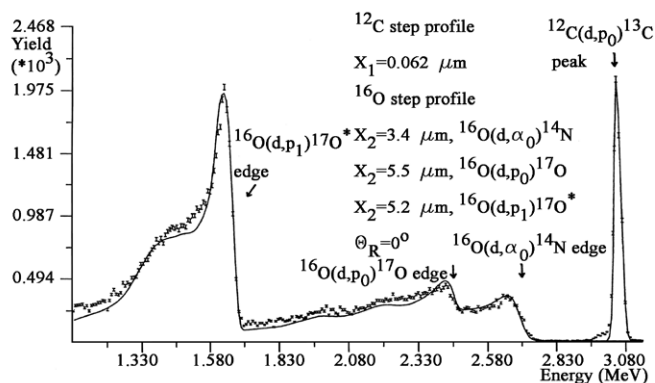


Fig. 5- Computed fit to data of the $^{12}\text{C}(d,p_0)^{13}\text{C}$, $^{16}\text{O}(d,p_0)^{17}\text{O}$, $^{16}\text{O}(d,p_1)^{17}\text{O}^*$ and $^{16}\text{O}(d,\alpha_0)^{14}\text{N}$ reactions in the quartz target, for $E_a=1.0$ MeV and $\theta_L=135^\circ$.

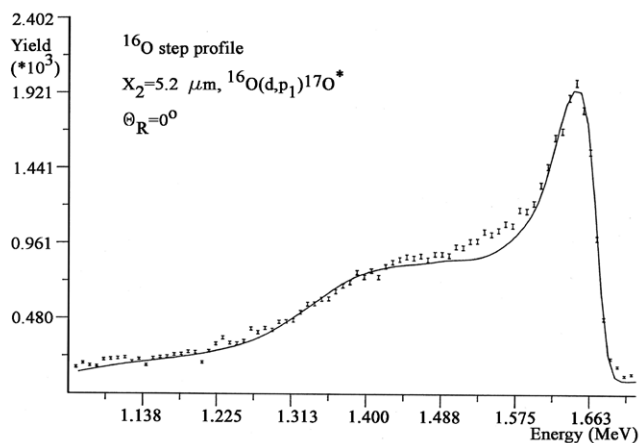


Fig. 6- Computed fit to data corresponding to the $^{16}\text{O}(d,p_1)^{17}\text{O}^*$ reaction peak in the quartz target, for $E_a=0.993$ MeV and $\theta_L=135^\circ$.

4.2. Elastic Scattering

In making the computer predictions for elastic scattering spectra of α particles we used available data of stopping power of α particles in the samples (21) and, unless otherwise stated, Rutherford differential cross sections.

4.2.1. Sapphire target

The sapphire target, labelled Al_2O_3 , was first analysed through a 1.5 MeV $(^4\text{He})^+$ ion beam at normal incidence. The corresponding elastic scattering spectrum, obtained at an angle of 165° , is shown in Fig. 7. A good computed fit to data was obtained for a ratio of atomic densities of O and Al ($C_{\text{O}}/C_{\text{Al}}$) of 1.500, corresponding to Al_2O_3 stoichiometry. However, the ratio mentioned must be interpreted with caution given the statistical errors in the Al and O spectral shapes. The accuracy is at best 2%, ignoring any inaccuracies in the stopping power. The same sample was also analysed at 3.105 MeV and 165° , as shown in Fig. 8. In this case, in making the predictions, we used the differential cross section data for elastic scattering of α particles in ^{16}O at 165° given in (31). These data exhibit a peak at 3.045 MeV, corresponding to resonant scattering. This peak provides for enhanced detection sensitivity of ^{16}O through elastic scattering of α particles. The predictions

resulted in a good fit to the data. For uniform concentration profiles of Al and O, thickness parameters of 1.89 and 1.21 μm were used, respectively.

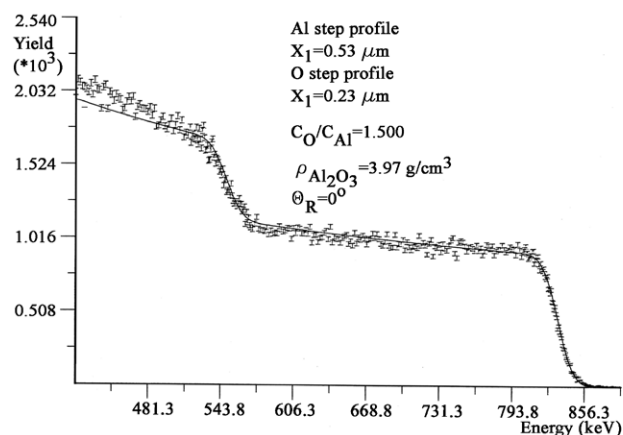


Fig. 7- Computed fit to data of elastic scattering of α particles in the sapphire target for $E_a=1.5$ MeV and $\theta_L=165^\circ$.

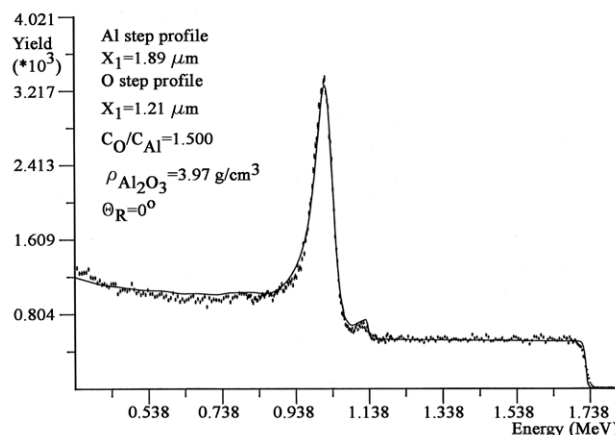


Fig. 8- Computed fit to data of elastic scattering of α particles in the sapphire target for $E_a=3.105$ MeV and $\theta_L=165^\circ$.

4.2.2. Al/ Al_2O_3 target

The sample designated as Al/ Al_2O_3 was analysed through a 2.0 MeV $(^4\text{He})^+$ ion beam, normal incidence and $\theta_L=165^\circ$. For the respective spectrum of elastic scattering of α particles, not shown, a good computed fit to data was obtained for an aluminium oxide film thickness of 0.1350 μm , which is very close to the value of 0.1340 μm determined through transmission electronic microscopy. The fit indicated that the ratio of atomic densities of O and Al is slightly higher than 1.500. The same sample was analysed at 1.5 MeV and 165° , at normal incidence and at a rotation angle of $20 \pm 1.5^\circ$. The corresponding computed fits are shown in Fig. 9 and Fig. 10, respectively. In both cases the predictions give reasonably good fits to the data for an aluminium oxide film thickness of 0.1370 μm , close to the values obtained at 2.0 MeV and measured through transmission electronic microscopy. These fits would be improved by using a ratio of atomic densities of O and Al ($C_{\text{O}}/C_{\text{Al}}$) of 1.530, within an accuracy of $\sim 2\%$, resulting in an oxide stoichiometry of $\text{Al}_2\text{O}_{3.06 \pm 0.06}$ close to $\text{Al}_2\text{O}_{3.05 \pm 0.05}$ given in (32).

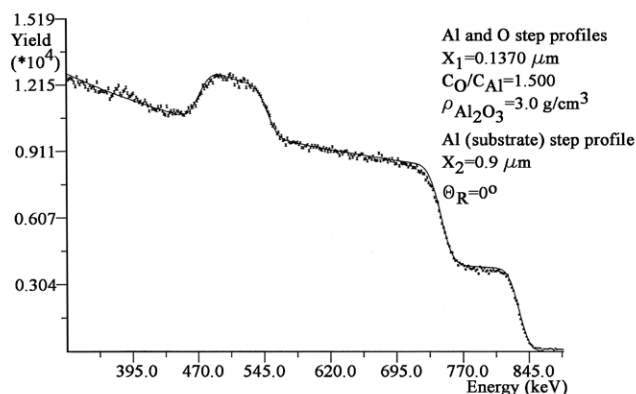


Fig. 9- Computed fit to data of elastic scattering of α particles in the Al/Al₂O₃ target for $E_\alpha=1.5$ MeV and $\theta_L=165^\circ$.

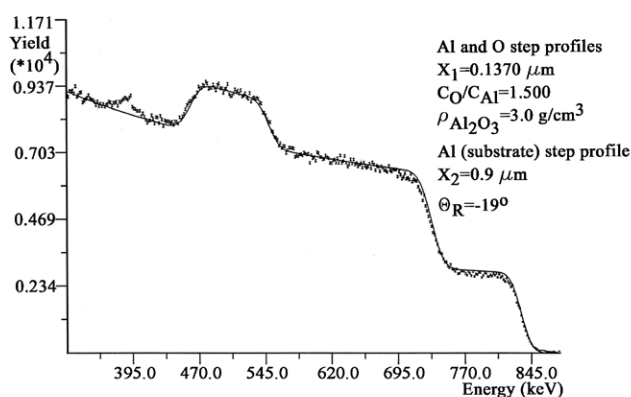


Fig. 10- Computed fit to data of elastic scattering of α particles in the Al/Al₂O₃ target for $E_\alpha=1.5$ MeV and $\theta_L=165^\circ$.

4.2.3. Self-supported targets

The self-supported samples of anodic aluminium oxide, which were obtained by aluminium anodization at 100V and 200V, were analysed with 2.0 MeV (4He)⁺ ion beams at normal incidence and detection angles of 165° and 135°. Several spectra of elastic scattering of α particles were acquired for each target. The integrated yields of the spectral shapes from O and Al were used to calculate the ratios of atomic densities C_O/C_{Al} . Several computed fits were made to the data. The values of the ratios of atomic densities of O and Al and oxide thicknesses were consistent, within the experimental error. For the target anodized at 100V the average values were $C_O/C_{Al} = 1.53 \pm 0.06$ and $X_1 = 0.1333 \mu\text{m}$. These values are in reasonably good agreement with those (1.53 and 0.1350 μm) obtained at 2.0 MeV for the Al/Al₂O₃ target, which was anodized at the same voltage. For the target anodized at 200V the average values were $C_O/C_{Al} = 1.52 \pm 0.07$ and $X_1 = 0.2480 \mu\text{m}$. While the ratio mentioned agrees reasonably well with the determinations for the targets anodized at 100V, the oxide thickness per volt (12.4 Å/V) is lower. A possible explanation for this would be that the 200V oxide film has undergone dissolution during formation. Dissolution and hydration of aluminium oxides obtained by anodization in

aqueous solutions of ammonium citrate have been reported (33). The computed fits which were made are illustrated by the fit shown in Fig. 11 for the 200V target, at 2.0 MeV and $\theta_L=135^\circ$. In this spectrum the spectral shapes of elastic scattering from Al and O are superimposed on a continuous background due to scattering always appearing in experiments involving self-supported targets. We managed to reduce it through the detector arrangement and by taking precautions about the configuration of the Faraday cup after the target chamber. After background subtraction, an improved and more reliable fit was made to the same data, using $C_O/C_{Al} = 1.523$, within an accuracy of ~4%, and the same oxide thickness $X_1 = 0.2460 \mu\text{m}$.

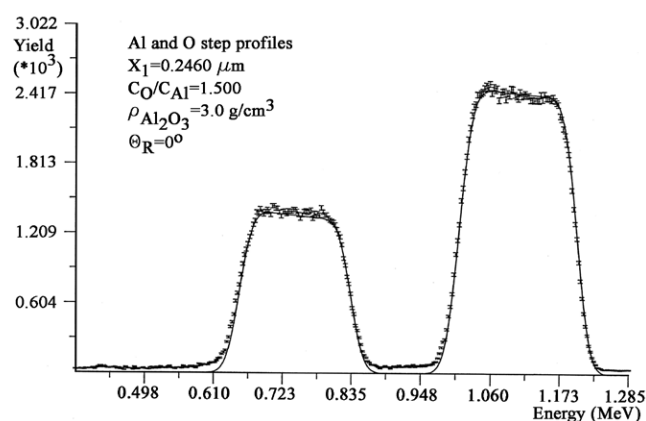


Fig. 11- Computed fit to data of elastic scattering of α particles in the 200V self-supported target of anodic aluminium oxide, for $E_\alpha=2.0$ MeV and $\theta_L=135^\circ$.

5. CONCLUSIONS

This work has given very positive, important and successful answers in problem areas of surface analysis by nuclear reactions, for depth profiling of ¹²C and ¹⁶O nuclei, and elastic scattering. The spectral predictions, made by computer simulation for nuclear reactions and elastic scattering, resulted in good descriptions of experimental spectra obtained for thick samples and considerable depths close to the surface, and for samples containing thin films of aluminium oxide. The nuclear techniques have shown to be very powerful analytical tools in this context. Several results here presented would be very difficult to obtain by non-nuclear techniques.

ACKNOWLEDGMENTS

We acknowledge the supports from Universidade da Beira Interior (UBI) and Fundação para a Ciência e a Tecnologia (FCT).

REFERENCES

1. J. F. Ziegler, Material analysis by nuclear backscattering-Introduction, in: New uses of ion accelerators, (J. F. Ziegler, (Ed)), Plenum Press, New York, 75-103 (1975).
2. G. Amsel, G. Battistig, The impact on materials science of ion beam analysis with electrostatic accelerators, Nucl. Instr. and Meth. B, 240, 1-12 (2005).
3. J. M. Calvert, D. J. Derry, D. G. Lees, Oxygen diffusion studies using nuclear reactions, J. Phys. D: Appl. Phys., 7, 940-953 (1974).

4. P. J. Wise, Ph. D. Thesis, University of Manchester, England, (1974).
5. P. J. Wise, D. G. Barnes, D. J. Neild, Measurement of atomic concentration profiles in thin films using nonresonant nuclear reactions, *J. Phys. D: Appl. Phys.*, 7, 1475-1481 (1974).
6. J. A. R. Pacheco de Carvalho, Ph. D. Thesis, University of Manchester, England, (1984).
7. J. A. R. Pacheco de Carvalho, J. M. Calvert, Surface analysis through the $^{18}\text{O}(\text{p},\alpha)^{15}\text{N}$ reaction, in: *Proc. Física 1994-9ª Conferência Nacional de Física*, (Sociedade Portuguesa de Física (Ed)), Universidade da Beira Interior, Covilhã, Portugal, 350-350 (1994).
8. Liao Changgeng, Jian Hui, Wang Yongqiang, Zheng Zhihao, Boron depth profiles in silicon and simulation of α -spectra, *Nucl. Instr. and Meth. B*, 95, 97-101 (1995).
9. J. R. Liu, Y. P. Li, Q. Y. Chen, X. T. Cui, R. Christoffersen, A. Jacobson, W. K. Chu, Depth resolution and dynamic range of $^{18}\text{O}(\text{p},\alpha)^{15}\text{N}$ depth profiling, *Nucl. Instr. and Meth. B*, 136-138, 1306-1311 (1998).
10. J. A. R. Pacheco de Carvalho, Surface analysis by nuclear techniques, in: *Proc. Física 2002-13ª Conferência Nacional de Física*, (Sociedade Portuguesa de Física-Norte (Ed)), Universidade de Évora, Évora, Portugal, 291-291 (2002).
11. J. A. R. Pacheco de Carvalho, Aplicações de técnicas nucleares e computacionais à análise de superfícies de materiais, in: *Proc. Engenharia'2003-Inovação e Desenvolvimento-2ª Conferência de Engenharia*, (Denis A. Coelho, Anna D. Guerman. (Eds)), Universidade da Beira Interior, Covilhã, Portugal, 494-499 (2003).
12. J. A. R. Pacheco de Carvalho, A. D. Reis, Simulação computacional e difusão elástica na análise de superfícies, in: *Proc. Física 2006-15ª Conferência Nacional de Física-Traçando o Futuro*, (Sociedade Portuguesa de Física-Delegação Regional Centro. (Ed)), Universidade de Aveiro, Aveiro, Portugal, FN3, 105-105 (2006).
13. J. A. R. Pacheco de Carvalho, A. D. Reis, Simulação Computacional e Técnicas Nucleares de Análise de Superfícies, in: *Proc. Física 2005-14ª Conferência Nacional de Física-Física para o Sec. XXI*, (Sociedade Portuguesa de Física-Norte (Ed)), Universidade do Porto, Porto, Portugal, 231-232 (2005).
14. G. Amsel, G. Béranger, B. de Gélas, P. Lacombe, Use of the nuclear reaction $^{16}\text{O}(\text{d},\text{p})^{17}\text{O}$ to study oxygen diffusion in solids and its application to zirconium, *J. Appl. Phys.*, 39, 5, 2246-2255 (1968).
15. S. Maroie, R. Caudano, G. Debras, J. Verbist, The use of prompt nuclear reactions and resonant alpha scattering in the study of α and β brass oxidation, *Appl. Surf. Sci.*, 4, 3-4, 466-480 (1980).
16. F. Freund, G. Debras, G. Demortier, Carbon content of high-purity alkaline earth oxide single crystals grown by arc fusion, *J. Am. Ceram. Soc.*, 61, 9-10, 429-434 (1978).
17. G. Debras, G. Deconninck, Light element analysis and application to glass industry, *J. Radioanal. Nucl. Chem.*, 38, 1-2, 193-204 (1977).
18. E. Rauhala, N. P. Barradas, S. Fazinic, M. Mayer, E. Szilágyi, M. Thompson, Status of ion beam data analysis and simulation software, *Nucl. Instr. and Meth. B*, 244, 436-456 (2006).
19. N.P. Barradas, K. Arstila, G. Battistig, M. Bianconi, N. Dytlewski, C. Jeynes, E. Kótai, G. Lulli, M. Mayer, E. Rauhala, E. Szilágyi, M. Thompson, International Atomic Energy Agency intercomparison of ion beam analysis software, *Nucl. Instr. and Meth. B*, 262, 282-303 (2007).
20. G. Amsel, Thesis, University of Paris, Faculty of Science, Orsay, (1963).
21. J. F. Ziegler, in: *The stopping and ranges of ions in matter: Helium stopping powers and ranges in all elements*, Vol.4, (J. F. Ziegler. (Ed)), Pergamon Press Inc., Oxford, (1977).
22. H. H. Andersen, J. F. Ziegler, in: *The stopping and ranges of ions in matter: Hydrogen stopping powers and ranges in all elements*, Vol.3, (J. F. Ziegler. (Ed)), Pergamon Press Inc., Oxford, (1977).
23. W. H. Bragg, R. Kleeman, On the α particles of Radium and their loss of range in passing through various atoms and molecules, *Phil. Mag.*, 10, 318-341 (1905).
24. N. Bohr, On the penetration of charged particles through matter, *Mat. Fys. Medd. Dan. Vid. Selsk.*, 18, 8, 1-144 (1948).
25. J. Lindhard, M. Scharff, Energy loss in matter by fast particles of low charge, *Mat. Fys. Medd. Dan. Vid. Selsk.*, 27, 15, 1-13 (1953).
26. E. Fermi, in: *Nuclear Physics*, The University of Chicago Press, Chicago, 36 (1950).
27. H. A. Bethe, J. Ashkin, in: *Experimental Nuclear Physics*, Vol. I, (E. Segrè. (Ed)), John Wiley and Sons, Inc., New York, 285 (1953).
28. D. C. Santry, R. D. Werner, Stopping power of C, Al, Si, Ti, Ni, Ag and Au for deuterons, *Nucl. Instr. and Meth.*, 188, 211-216 (1981).
29. C. F. Williamson, J. P. Boujot, J. Picard, Tables of range and stopping power of chemical elements for charged particles of energy 0.05 to 500 MeV, *Tech. Rept. N° C. E. A.-R 3042*, Centre d'Études Nucleaires de Saclay, (1966).
30. G. Debras, Thesis, Facultés Universitaires de Namur, Belgium, (1977).
31. R. A. Jarjis, *Nuclear Cross Section Data for Surface Analysis*, vols 1, 2 e 3, Department of Physics, University of Manchester, England, (1979).
32. A. L. Hoir, C. Cohen, G. Amsel, Experimental study of the stopping power and energy straggling of MeV ^4He , ^{12}C , ^{14}N and ^{16}O ions in amorphous aluminium oxide, in: *Ion beam surface layer analysis- Proc. 2nd Int. Conf. Ion Beam Surf. Layer Anal.*, Karlsruhe, 1975, Vol. 2, (O. Meyer, G. Linker, F. Käppeler. (Eds)), Plenum Press, New York, 965-976 (1976).
33. J. A. Davies, T. E. Jackman, H. Plattner, I. Bubb, Absolute calibration of $^{14}\text{N}(\text{d},\alpha)$ and $^{14}\text{N}(\text{d},\text{p})$ reactions for surface adsorption studies, *Nucl. Instr. and Meth.*, 218, 1-3, 141-146 (1983).

Recibido: 31.07.07
 Aceptado: 20.12.07




www.secv.es

Sociedad Española de Cerámica y Vidrio

Archivo Edición Ver Favoritos Herramientas Ayuda


← Atrás → Búsqueda Favoritos Multimedia

Dirección http://www.secv.es Ir Vínculos »



SOCIEDAD ESPAÑOLA DE CERAMICA Y VIDRIO

- Abstracts ☐
- ¿Qué es la SECV? ☐
- Organigrama ☐
- Secciones ☐
- Congresos ☐
- Publicaciones ☐
- Rel. Institucionales ☐
- Premios Alfa de Oro ☐
- Solicitud de afiliación ☐



Centro Cultural
c/ Ferraz, 11 3º dcha. 28080 Madrid
Tfno.: +34 - 91 735 58 40 ext.: 1176 / 1177
Fax: +34 - 91 735 58 43

Sede Social
Instituto de Cerámica y Vidrio
Despacho 176
Camino de Valdelatas s/n 28049 Madrid, Spain
Tlf: +34 - 91 735 58 40 extensiones: 1176 / 1177
Directo: 91 735 58 60; Fax: +34 - 91 735 58 43
web: secv.es; e-mail: secv@icv.csic.es

www.secv.es

Sociedad Española de Cerámica y Vidrio

Congresos Anuales de la SECV

- Abstracts
- ¿Qué es la SECV?
- Organigrama
- Secciones
- Congresos**
- Congresos Anuales de la SECV
- Congresos Internacionales organizados por la SECV
- Exposiciones
- Publicaciones
- Rel. Institucionales
- Premios Alfa de Oro
- Solicitud de afiliación

Nº	Título del Congreso	Lugar y Fecha
IV	SEMANA ESTUDIOS CERAMICOS	Madrid, 24-28 Abril 1962
V	SEMANA ESTUDIOS CERAMICOS	Madrid, 7-10 Mayo 1963
VI	SEMANA ESTUDIOS CERAMICOS	Madrid, 11-15 Mayo 1964
VII	SEMANA ESTUDIOS CERAMICOS	Madrid, 17-20 Mayo 1965
VIII	SEMANA ESTUDIOS CERAMICOS	Madrid, 1-4 Junio 1966
VIII	CONGRESO ANUAL SECV Con la colaboración de: Facultad de Ciencias de la Universidad de Sevilla y Sociedad Francesa de Genetique	Sevilla, 10-13 Mayo 1967
IX	CONGRESO ANUAL SECV Con la colaboración de: Escuela Técnica Superior de Ingenieros Industriales. San Sebastian, Universidad de Navarra.	San Sebastian, 5-8 Octubre 1968
X	CONGRESO ANUAL SECV Con la colaboración de: Universidad de Zaragoza	Zaragoza, 27-30 Sept. 1970
XI	CONGRESO ANUAL SECV Con la colaboración de: Universidad de Granada; Sociedad Española de Arcillos	Granada, 5-8 Octubre 1971

SOCIEDAD ESPAÑOLA DE CERAMICA Y VIDRIO